A Truncated Polycystin-2 Protein Causes Polycystic Kidney Disease and Retinal Degeneration in Transgenic Rats

Anna Rachel Gallagher,* Sigrid Hoffmann,† Nelson Brown,* Anna Cedzich,*† Sujatha Meruvu,* Dirk Podlich,† Yuxi Feng,‡ Vera Könecke,* Uwe de Vries,* Hans-Peter Hammes,‡ Norbert Gretz,† and Ralph Witzgall*

**Institute for Molecular and Cellular Anatomy, University of Regensburg, Regensburg, and †Medical Research Center and ‡Department of Internal Medicine V, Klinikum Mannheim, University of Heidelberg, Mannheim, Germany*

The cloning of the *PKD1* and *PKD2* genes has led to promising new insight into the mechanisms that are responsible for cyst development in patients with autosomal dominant polycystic kidney disease. Although the dominant pattern of inheritance would argue for haploinsufficiency, a gain of function, or a dominant negative mechanism, there is good evidence that autosomal dominant polycystic kidney disease behaves like a recessive disease on a cellular level (two-hit mechanism of cystogenesis). For testing of whether other pathomechanisms in addition to the two-hit hypothesis can explain cyst formation, two transgenic rat lines that contain a truncated human polycystin-2 cDNA were generated. The protein product lacks almost the entire COOH-terminus and mimics mutations that frequently are found in patients. The transgene-encoded mRNA could be detected in multiple tissues of both transgenic lines, with the highest expression in the kidney. Both lines present with renal cysts that originate predominantly from the proximal tubule; in the tubular epithelial cells, the epitope-tagged mutant protein was detected in the brush border and in primary cilia. Further evidence of the involvement of primary cilia stems from the finding of retinal degeneration in the transgenic rats and from the fact that stably transfected LLC-PK$_1$ cells that inducibly produced the truncated polycystin-2 protein elaborated shorter cilia. Other experimental approaches, such as a knock-in strategy, will be necessary to validate these results, but this is the first preliminary evidence that cyst formation is due not only to somatic mutations.

J Am Soc Nephrol 17: 2719–2730, 2006. doi: 10.1681/ASN.2005090979

At a prevalence of at least 1:1000 (1,2), autosomal dominant polycystic kidney disease (ADPKD) is the most common hereditary renal disorder. It is characterized by the growth of numerous fluid-filled cysts within the parenchyma of the kidney, which eventually leads to the loss of renal function, such that approximately 50% of affected individuals develop end-stage renal failure by the age of 60 (3–5). A high number of apoptotic figures in cyst-lining epithelial cells, increased mitotic rates, and cyst formation in transgenic mice that produce cell cycle–promoting proteins suggest that an imbalance between cell proliferation and apoptosis plays a role in cyst formation. Other abnormalities that are found in cyst wall epithelia include a change in cell polarity, aberrant fluid secretion, and a dysregulated synthesis of metalloproteinases and tissue inhibitors of metalloproteinases (for review, see reference [6]).

Genetically, ADPKD is a heterogeneous disease; in approximately 85% of patients, it is caused by mutations in the *PKD1* gene, and in approximately 15% of patients, it is caused by mutations in the *PKD2* gene (7–10). Polycystin-2, the protein that is encoded by the *PKD2* gene, is a 968–amino acid protein with six putative transmembrane domains; sequence homology to voltage-activated calcium channels and to the Trp family of calcium channels suggested already early on that it functions as an ion channel (11). This hypothesis indeed was proved correct later by patch-clamp and single-channel recordings that showed that polycystin-2 functions as a high-conductance, nonselective cation channel (for review, see reference [12]). So far, most of the biochemical information is available on the COOH-terminus of polycystin-2, which has been shown to interact with polycystin-2 itself (13,14) and with α-actinin (15), CD2AP (16), mDia1 (17), Id2 (18), the inositol-1,4,5-triphosphate (IP_3) receptor (19), phosphofurin acidic cluster sorting protein–1 (PACS-1) and PACS-2 (20), polycystin-2 interactor, Golgi- and endoplasmic reticulum–associated protein–14 (PIGEA-14) (21), polycystin-1 (13,14), tropomyosin-1 (22), troponin I (23), and transient receptor potential-canonical (TRPC1) (24). The intracellular location of polycystin-2 is a matter of intense debate: Not only arguments for its location in the endoplasmic reticulum and the plasma membrane have been put forward (25), but

Received September 21, 2005. Accepted July 21, 2006.

Published online ahead of print. Publication date available at www.jasn.org.

A.R.G.'s current affiliation is Department of Internal Medicine, Yale University School of Medicine, New Haven, CT. N.B.'s current affiliation is Molecular Oncology Research Institute, Tufts-New England Medical Center, Boston, MA. A.C.'s current affiliation is Institute of Plant Physiology and Biotechnology, University of Hohenheim, Stuttgart, Germany.

A.R.G., S.H., and N.B. contributed equally to this work.

Address correspondence to: Ralph Witzgall, University of Regensburg, Institute for Molecular and Cellular Anatomy, Universitätsstraβe 31, 93053 Regensburg, Germany. Phone: +49-0-941-943-2821; Fax: +49-0-941-943-2868; E-mail: ralph.witzgall@vkl.uni-regensburg.de

ISSN: 1046-6673/1710-2719

also, more recently, polycystin-2 has been detected in the primary cilium of renal epithelial cells (26,27).

One puzzling observation in the field concerns the fact that ADPKD is inherited in a dominant manner, but cysts develop only in a limited number of nephrons. This phenomenon has been explained by the finding that cyst-lining cells suffer from a somatic mutation in the allele of the respective *PKD* gene that is not mutated in the germline. On a cellular level, ADPKD therefore can be considered a recessive disease (for review, see reference [28]). The two-hit model of cyst formation has been supported further by a *Pkd2* mutant mouse in which the somatic rearrangement of an unstable allele to a null allele leads to cyst formation (29,30). However, a mutation in the second allele of the same gene or in the alternate gene (a phenomenon called *trans*-heterozygosity [31,32]) has not been found in 100% of the investigated cysts, which may be due to the technically challenging protocol of detecting mutations in very few cells or because an additional pathway of cystogenesis exists. Because many mutations in patients with ADPKD are predicted to lead to the synthesis of a truncated protein, we decided to generate transgenic rats that produce an epitope-tagged mutant polycystin-2 protein that lacks almost the entire COOH-terminus. In this study, we describe the phenotypic consequences in these animals.

Materials and Methods

Expression Plasmids

The full-length human PKD2 cDNA (gift from Stefan Somlo, Yale University School of Medicine, New Haven, CT) was cloned into the KpnI/XbaI sites of pUC18. With the use of a PCR-based strategy, a fragment that encoded an epitope from the influenza virus hemagglutinin protein (HA-epitope) was inserted immediately upstream of the stop codon. During the construction, the BsaAI site before the stop codon was deleted, and an XhoI site was placed between the HA-coding sequence and the stop codon. The sequence of the resulting construct PKD2, HA reads as follows (the last three codons of PKD2 are boldface; the sequence encoding the HA-epitope is italicized): 5′-. . . **GTC CAC GTC** *TAC CCA TAC GAT GTT CCA GAT TAC GCT* CTC GAG TGA. . . -3′.

An analogous strategy was used to tag the polycystin-2 protein at the COOH-terminus with a tail of six histidines. A ClaI site was introduced after the last PKD2 codon, and again the BsaAI site before the stop codon was deleted and an XhoI site was inserted between the His_6-encoding sequence and the stop codon. The sequence of the resulting construct PKD2, His reads as follows (the last three codons of PKD2 are boldface; the sequence encoding the 6 histidines is italicized): 5′-. . . **GTC CAC GTC** ATC GAT CGC GGC TCC *CAC CAC CAC CAC CAC CAC* CTC GAG TGA. . . -3′.

An HA-epitope–tagged mutant of the polycystin-2 protein that extended from amino acids 1 to 703 was created using an internal BglII site in the PKD2 cDNA and an adaptor. During the construction, an AflII site was placed between the PKD2 sequence and the sequence that codes for the HA-epitope. The sequence of the resulting construct PKD2 (1–703), HA reads as follows (the last three codons of PKD2 are boldface; the sequence encoding the HA-epitope is italicized): 5′-. . . **TCA GAT CTT** CTT AAG *TAC CCA TAC GAT GTT CCA GAT TAC GCT* TAA. . . -3′.

The PKD2, HA; the PKD2, His; and the PKD2 (1–703), HA fragments were inserted into the eukaryotic expression plasmid pUHD 10-3 (gift from H. Bujard, Zentrum für Molekulare Biologie der Universität Heidelberg, Heidelberg, Germany). The correct orientation of the insert was confirmed by restriction enzyme digestion and DNA sequencing.

Generation of Transgenic Rats, Genotype Analysis, and Urine and Serum Chemistry

A 2.2-kbp cDNA fragment that encoded the HA-epitope–tagged truncated human polycystin-2 protein extending from amino acids 1 to 703 was subcloned into a plasmid that was designed specifically for the generation of transgenic animals. This plasmid, pUCTrans, contains a cytomegalovirus (CMV) promoter upstream and the intron and polyadenylation signal of SV40 downstream of an EcoRI cloning site (Figure 1a). The transgenic cassette was removed from the plasmid using ClaI and ApaLI, purified over an Elutip-D column (Schleicher and Schuell, Dassel, Germany), and injected into the pronuclei of fertilized oocytes that were harvested from Sprague-Dawley rats. Genomic DNA was isolated from rat tails and subjected to Southern blot analysis according to standard protocols (33). For detection of the transgene, 10 μg of genomic DNA was digested with BamHI and hybridized with a radiolabeled 1.0-kbp BamHI fragment of the human PKD2 cDNA. For urine and serum chemistry, individual rats were placed in metabolic cages for 24 h to determine the daily urinary excretion of total protein and albumin. Blood samples were taken in parallel for serum creatinine and urea measurements. The rats received standard rat diet (containing 19% protein) and had free access to tap water. All experiments were conducted in accordance with the German Animal Protection Law and were approved by the local government (Regierungspräsidium Karlsruhe, Germany).

Cell Culture and Transfections

HtTA-1 cells (HeLa cells that express the tetracycline-controlled transactivator; gift from H. Bujard) (34) and LtTA-2,22 cells ($LLC\text{-}PK_1$ cells that express the tetracycline-controlled transactivator) (35) were cultured in DMEM with 10% FCS, 200 μg/ml G418 (Life Technologies, Karlsruhe, Germany), and 10 ng/ml (unless otherwise indicated) of doxycycline (Sigma, Taufkirchen, Germany) to prevent the synthesis of the protein of interest (tet-off system). For stable transfections, cells were seeded into 25-cm^2 flasks. When the cells had reached approximately 70% confluence, they were transfected with 8 μg of the expression plasmids pUHD 10-3/PKD2, HA or pUHD 10-3/PKD2 (1–703), HA, respectively, as well as with 0.8 μg of the selection plasmid pBabe Puro (36) by using a calcium phosphate protocol (37). Sixteen hours after the addition of the DNA, the cells were split onto 100-mm petri dishes; 2 d later, the selection process was initiated with 0.5 μg/ml of puromycin (Calbiochem, Schwalbach, Germany). Individual colonies were isolated and tested for the inducible expression of the full-length and truncated polycystin-2 proteins.

Stably transfected HeLa cell lines that coexpressed either the full-length and truncated polycystin-2 proteins or two differently tagged full-length polycystin-2 proteins were established as follows. HtTA-1 cells that inducibly expressed the HA-epitope–tagged full-length or truncated polycystin-2 proteins were co-transfected with the expression plasmid pUHD10-3/PKD2, His and the selection plasmid pWE4 (38) according to the poly-L-ornithine method (39). The selection was started 72 h later with the addition of 300 μg/ml of hygromycin (Calbiochem). Resistant colonies were isolated and tested for the inducible expression of the His-tagged full-length polycystin-2 protein.

Calcium Measurements

$LLC\text{-}PK_1$ cells were grown for 6 d in the presence and absence of 1 μg/ml of doxycycline before being transferred onto coverslips. Two to

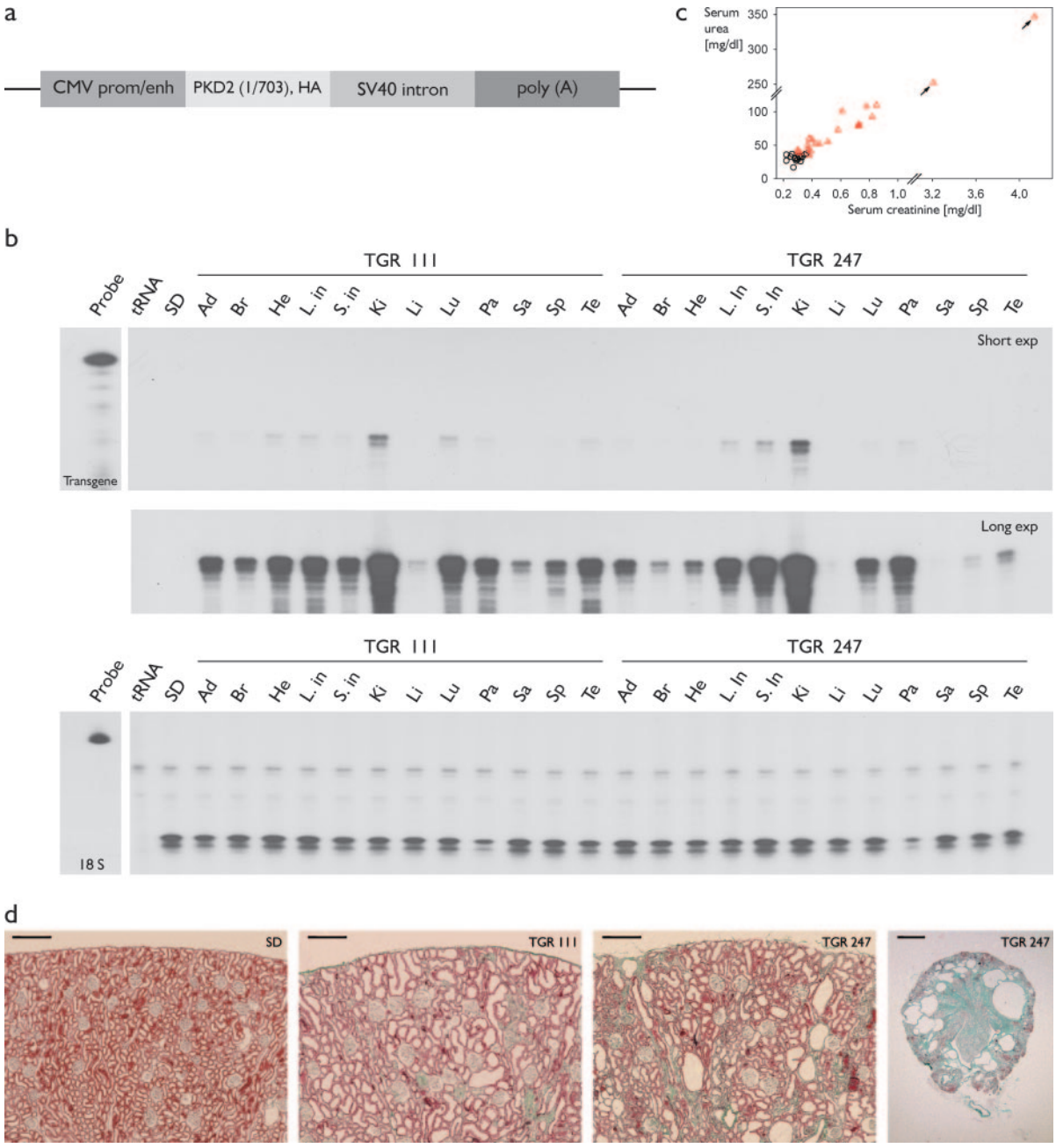

Figure 1. Transgenic rats with a truncated polycystin-2 protein develop polycystic kidney disease. (a) Schematic description of the transgenic expression cassette (not drawn to scale; total length of the injected fragment was approximately 3.6 kbp). The cytomegalovirus (CMV) promoter/enhancer region controls the synthesis of a truncated human polycystin-2 protein of 703 amino acids in length and an hemagglutinin protein (HA)-epitope at its COOH-terminus [PKD2 (1/703), HA]. To enhance the expression of the cDNA, an intron and polyadenylation signal [poly(A)] of SV40 were inserted at the 3′ end of the cassette. (b) The transgene-encoded mRNA was detected by RNase protection assay with a probe directed against the 3′-untranslated region (its specificity can be appreciated by the fact that no signal was detected in the kidney of a normal Sprague-Dawley rat [SD]). After an 8-h exposure (Short exp), a clear signal can be seen in the kidneys of both transgenic rats 111 and 247 (TGR 111 and TGR 247), whereas after a 14-d exposure (Long exp), the widespread expression of the transgene becomes evident (top two panels). A RNase protection assay for the 18S RNA shows that the RNA concentrations were determined correctly; tRNA served as a negative control. Ad, adrenal gland; Br, brain; He, heart; L. in, large intestine; S. in, small intestine; Ki, kidney; Li, liver; Lu, lung; Pa, pancreas; Sa, salivary gland; Sp, spleen; Te, testis. (c) Serum creatinine and urea concentrations in wild-type rats (○) and rats of transgenic line 247 (△). Animals between 7 and 12 mo old were used for serum analysis except for the two 15-mo-old rats indicated by arrows. (d) Sections through the kidneys of a normal SD rat and of both transgenic rat lines (TGR 111, TGR 247) were stained with Goldner's trichrome stain to demonstrate fibrotic tissue (green). The middle panels show typical cortical sections of 5-mo-old transgenic rats, whereas the one on the far right shows a whole-kidney section from a 3-mo-old rat with pronounced focal cyst formation and accompanying fibrosis. Bars = 400 μm (cortical sections in the first three panels) and 2 mm (whole kidney on the far right).

4 d after the cells were plated onto coverslips, they were washed twice in imaging buffer that contained 150 mM NaCl, 5 mM KCl, 2.2 mM $CaCl_2$, 5 mM glucose, 10 mM HEPES (pH 7.4), and 1 mM $MgCl_2$. Subsequently, the cells were loaded for 30 min at room temperature in imaging buffer to which 5 mM probenecid, 0.025% Pluronic (Invitrogen, Karlsruhe, Germany), and 5 μM Fura-2 AM (Invitrogen) were added. For stimulation of the cells with 10 μM ATP, the cells were washed twice with imaging buffer that contained probenecid and then incubated for at least 15 min in the same buffer before the fluorescence measurements started. For stimulation of the cells with ionomycin, the cells were washed twice after loading with imaging buffer that contained probenecid and incubated for at least 15 min in the same buffer before new imaging buffer that lacked Ca^{2+} but contained 2 mM EGTA was added. Once the fluorescence had stabilized, ionomycin was added to a final concentration of 10 μM. Fluorescence was measured by alternating between the excitation wavelengths of 340 and 380 nm and determining the emission every second for 10 min. Each curve represents measurements that were taken from eight coverslips that comprised 573 to 666 individual cells when cells were stimulated with ATP, and from four to six coverslips that comprised 278 to 464 individual cells when cells were exposed to ionomycin. Statistical significance of the difference between the peak $[Ca^{2+}]_i$ was calculated by subjecting the values to a *t* test.

Immunostaining and Histologic Staining of Tissues and Cells

Rats were perfused through the distal abdominal aorta with 4% paraformaldehyde and 1× PBS for 3 min at a pressure of 200 mmHg. Organs of interest were removed and immersed in 18% sucrose and 1× PBS before being frozen in liquid nitrogen or postfixed overnight in 4% PFA and 1× PBS for paraffin embedding. The following primary antibodies were used on cryosections: A mouse monoclonal anti-rat dipeptidyl peptidase IV antibody (40) (diluted 1:1000; gift from Werner Reutter, Institute of Molecular Biology and Biochemistry, Free University of Berlin, Berlin, Germany), a rabbit polyclonal anti-HA antibody (diluted 1:1000; Sigma), and a mouse monoclonal anti-acetylated α-tubulin antibody (diluted 1:200; Sigma). The following primary antibodies were used on microwave-treated, paraffin-embedded sections: A mouse monoclonal anti-HA antibody (diluted 1:100; Santa Cruz Biotechnology, Santa Cruz, CA), a mouse monoclonal anti–Na^+/K^+-ATPase antibody (diluted 1:200; Sigma), a mouse monoclonal anti–proliferating cell nuclear antigen antibody (diluted 1:100,000; Sigma), the mouse polyclonal anti–polycystin-2 antibody YCC2 (41) (diluted 1:5000; gift from Stefan Somlo and Yiqiang Cai, Yale University) and a mouse monoclonal anti–Sat-1 antibody (42) (diluted 1:100; gift from Birgitta Burckhardt, Zentrum Physiologie und Pathologie, Georg-August-Universität, Göttingen, Germany). Primary antibodies were incubated overnight at 4°C, then the sections were rinsed three times in PBS and incubated with a Cy3- or FITC-coupled secondary antibody (1:300; Dianova, Hamburg, Germany) for 1 h at room temperature. After washing in PBS, sections were mounted in bicarbonate-buffered glycerol and visualized using the Zeiss laser confocal microscope LSM 510 Meta (Göttingen, Germany). When genomic DNA was to be visualized, sections were incubated with 100 ng/ml of 4′,6-diamidino-2-phenylindole dihydrochloride as well. For Goldner's trichrome and for hematoxylin and eosin staining, paraffin sections were deparaffinized and treated according to standard protocols.

Stably transfected LLC-PK_1 cells were cultured on coverslips for at least 2 d. After fixation with Bouin's solution (0.1 M sodium phosphate [pH 7.4], 15% saturated picric acid, and 2% formaldehyde) for 20 min, the cells were permeabilized in 1× PBS, 2% BSA, and 0.1% Triton X-100 for 45 min and then incubated with the rabbit polyclonal anti-HA and the mouse monoclonal anti-acetylated tubulin antibodies for 2 h at room temperature. After three washes with 1× PBS, the cells were incubated with the FITC- and Cy3-conjugated secondary antibodies for 1 h at room temperature. Subsequently, the cells were washed with 1× PBS and mounted in bicarbonate-buffered glycerol. Pictures again were taken with the Zeiss laser confocal microscope LSM 510 Meta.

Scanning Electron Microscopy

For scanning electron microscopy, rats were perfused with 2% glutaraldehyde and 1× PBS for 3 min at a pressure of 200 mmHg. After the kidneys were postfixed in the same solution overnight, they were dehydrated in increasing concentrations of acetone. Once the tissues were equilibrated in 100% acetone, they were critical point–dried, spudder-coated with gold, and finally imaged in a Zeiss DSM 940 A scanning electron microscope.

Preparation of Total RNA and RNase Protection Assay

Organs of interest were removed rapidly, and total RNA was extracted according to the acid guanidinium-phenol-chloroform protocol (43). RNA concentration was measured photometrically at 260 nm, and integrity of the extracted RNA was checked by agarose gel electrophoresis. RNase protection analysis was performed according to standard protocols (33). A 180-bp fragment from the 3′-untranslated region and a 179-bp fragment from the 3′-coding region of the transgene, both of which do not cross-react with the endogenous rat Pkd2 mRNA; a 181-bp fragment of the rat Pkd2 cDNA; and an 80-bp 18S cDNA fragment (Ambion, Austin, TX) were used for *in vitro* transcription with ^{32}P-UTP. Twenty-five micrograms of total RNA was hybridized with the radiolabeled mRNA-specific riboprobes, whereas 25 ng of total RNA was hybridized with the radiolabeled 18S riboprobe; tRNA served as a negative control. The expression levels of the transgene and of the endogenous rat *Pkd2* gene were compared by scanning the dried polyacrylamide gels with a Fuji Image Reader FLA-5000 (Raytest GmbH, Staubenhardt, Germany), processing the scans with ImageJ software (W.S. Rasband, National Institutes of Health, Bethesda, MD; http://rsb.info.nih.gov/ij/), and normalizing the obtained values to the number of uridines in the riboprobes.

Immunoprecipitation

Cells were washed twice with 1× PBS and lysed in buffer that contained 1% Triton X-100, 0.05% SDS, 150 mM NaCl, 10 mM Tris-HCl (pH 7.5), 2 mM EDTA (pH 8.0), 1 μg/ml of leupeptin, and 1 mM PMSF. After centrifuging for 5 min at 14,000 rpm, the protein concentration was determined according to an improved Bradford assay (44) using the Protein Assay Kit from BioRad (Munich, Germany). For immunoprecipitation, the indicated amounts of total protein were incubated for 90 min at 4°C with 50 μl of supernatant from the 12CA5 hybridoma. Then 25 μl of swollen protein A–Sepharose beads was added to precipitate the immune complexes, followed by further incubation for 90 min at 4°C. Subsequently, the beads were washed twice with lysis buffer, resuspended in 50 μl of 1× SDS sample buffer (125 mM Tris-HCl [pH 6.7], 2.5% SDS, 10% glycerol, 2.5% β-mercaptoethanol, and 0.01% bromophenol blue), and incubated on ice for 30 min to elute the precipitated proteins from the beads.

SDS-PAGE and Western Blotting

Proteins were separated on denaturing polyacrylamide gels without previous boiling. The electrophoretic transfer of proteins from the gel onto a polyvinylidene difluoride membrane (Millipore, Eschborn, Germany) was carried out in a buffer that contained 50 mM Tris-HCl, 384 mM glycine, 20% methanol, and 0.1% SDS. After the transfer, the

membrane was blocked overnight at room temperature in blocking solution (5% low-fat dry milk powder, 0.05% Tween 20, and 1× PBS) and then incubated for 2 h with the primary antibody. The following primary antibodies were used: The mouse monoclonal anti–HA-epitope antibody 12CA5 (diluted 1:25) and a mouse monoclonal anti–His-epitope antibody (diluted 1:300; Roche Molecular Biochemicals, Mannheim, Germany). After two washes with 0.5% Tween 20 in 1× PBS and two washes with blocking solution, the membrane was incubated for 1 h with the horseradish peroxidase–conjugated anti-mouse IgG secondary antibody (diluted 1:10,000; Sigma). To detect the blotted proteins, we used a chemiluminescence detection kit (NEN Life Science, Köln, Germany).

Quantification of Cilia Length

The length of cilia was measured using the ImageJ software package.

Statistical Analyses

Statistical evaluations were performed using the TTEST procedure of the statistical analysis system (SAS) from SAS Institute (Cary, NC).

Results

Synthesis of a Truncated Polycystin-2 Protein in Transgenic Rats Leads to Renal Cyst Formation

We wanted to test whether additional mechanisms other than a somatic mutation play a role in cyst formation by expressing a truncated human PKD2 cDNA in transgenic rats, which were preferred over mice because they permit an easier physiologic characterization. To this end, we have generated two independent lines of transgenic Sprague-Dawley rats (line 111 and line 247) that synthesize a mutant polycystin-2 protein that lacks the region beyond amino acid 703. This particular polycystin-2 mutant was chosen because it lacks almost the entire region of polycystin-2 extending into the cytoplasm (the last membrane-spanning domain is predicted to end with amino acid 679) and because several mutations that affect this area were found in patients (45). Because the truncated protein was tagged with an HA-epitope, it could be discerned easily from the endogenous wild-type protein. The expression of the transgene was controlled by the promoter/enhancer region of the human CMV (Figure 1a), which is known for its strong activity in a wide variety of tissues. Indeed, the transgene-encoded mRNA was detected in many organs, although in both lines the highest levels were produced in the kidneys (Figure 1b). Line 247 showed slightly higher expression levels of the transgene, which may be because, according to Southern blot analysis, line 111 carried approximately two copies and line 247 carried approximately five copies of the transgene (data not shown). By RNase protection assay, we determined that in line 247 the kidneys contained approximately 15-fold and the eyes (see below) approximately seven-fold higher levels of the transgene-encoded mRNA than of the endogenous mRNA (data not shown). As a first characterization, transgenic rats at 3 mo of age were subjected to urine and serum analysis. In comparison with age-matched Sprague-Dawley rats, the serum creatinine concentration was significantly higher in line 247 and the urinary excretion of total protein and albumin in line 111; all other comparisons did not reach statistical significance (data not shown). This trend toward renal insufficiency progressed when the rats became older, and it became particularly evident in two rats at 15 mo of age (Figure 1c). Renal damage can be due to glomerular or tubular injury, and we therefore took a closer look at the kidneys. Upon histologic examination by Goldner's trichrome staining, cystically dilated tubules were found predominantly in the renal cortex of both transgenic lines (Figure 1d). In agreement with the serum and urine analysis, which showed some variability between rats, the degree of cyst formation between rats of the same age varied. It was surprising to see that in some kidneys, cysts obviously arose focally (Figure 1d). The trichrome staining also demonstrated a fibrotic remodeling of the kidneys that became very pronounced already at a relatively young age in some rats (Figure 1d). No pathologic changes were recognized in adrenal gland, brain, heart, large and small intestine, liver, lung, salivary gland, spleen, and testis.

The preponderance of cyst formation in the renal cortex suggested that most cysts developed in proximal tubules. Using an antibody against the brush border enzyme dipeptidyl peptidase IV, we were able to demonstrate that the majority of cysts indeed originated from this nephron segment. Neither dipeptidyl peptidase IV nor the basolateral proteins Na^+/K^+-ATPase and Sat-1 were reproducibly missorted (Supplemental Figure 1), thus arguing against a global change in cell polarity as causing cyst formation. Furthermore, with the exception of cysts in fibrotic areas (Supplemental Figure 2c), no obvious difference in the proliferation rate could be detected between proximal tubular and cyst-lining cells of transgenic rats and proximal tubular cells of control rats (Supplemental Figure 2, a and b). These data indicate that in our model, cell proliferation does not contribute substantially to cystogenesis.

Truncated Polycystin-2 Protein Affects Cilia Formation in Renal Epithelial Cells

If the formation of cysts in the transgenic rats occurred in a cell-autonomous manner, then the truncated polycystin-2 protein should be produced at the site of cyst formation (*i.e.*, in proximal tubules). Immunohistochemistry with the anti–HA-epitope antibody showed this to be the case. In normal and cystic profiles, the brush border of many but not all proximal tubules was labeled prominently for the truncated polycystin-2 protein; in cysts, the staining sometimes was seen in a mosaic manner, indicative of the loss of brush border in certain areas of the cysts (Figures 2a and 4d). Because it has been shown that the wild-type polycystin-2 protein is present in the primary cilium, we also double stained sections of the transgenic rat kidneys with the anti–HA-epitope antibody and an antibody against acetylated tubulin, a marker of primary cilia. It could be seen clearly that the truncated polycystin-2 protein also traffics to the primary cilium (Figure 2b). To corroborate our results in the transgenic rats, we examined stably transfected LLC-PK_1 cells that produced the same epitope-tagged truncated polycystin-2 protein. In LLC-PK_1 cells, we could find a strong staining of the primary cilium, consistent with the pattern in the transgenic rat kidneys (Figure 2c).

It has been speculated that primary cilia serve a mechanosensory role in the renal tubules and that by this mechanism, the

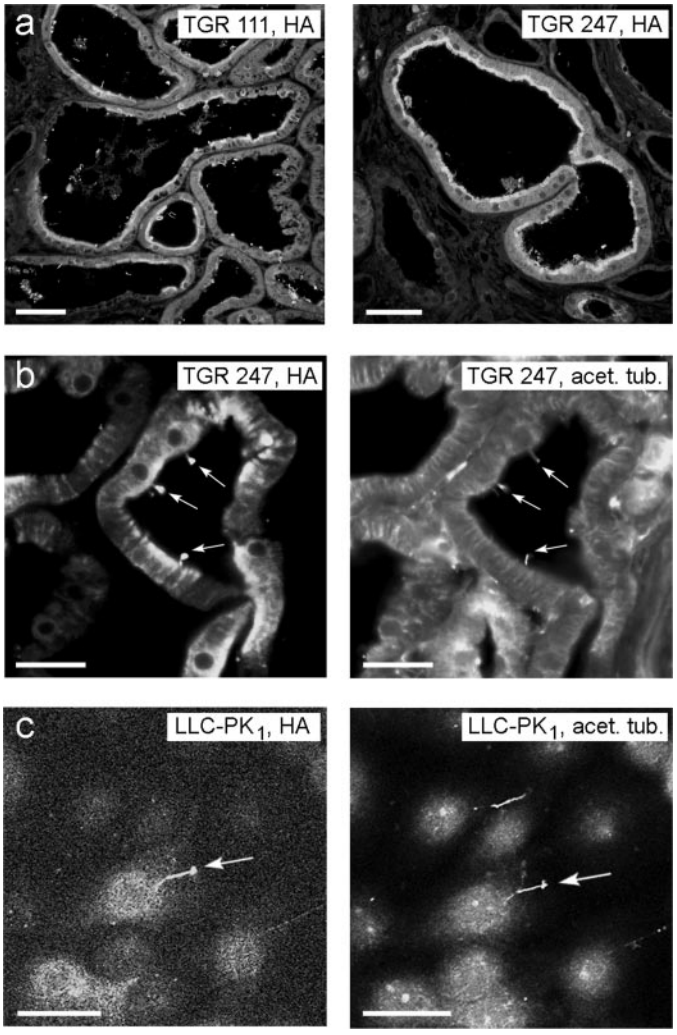

Figure 2. Localization of the truncated polycystin-2 protein. (a) The HA-epitope–tagged truncated polycystin-2 protein was detected on kidney sections by staining with the anti–-HA-epitope antibody. In both transgenic lines, the protein is present in the brush border. (b) Double staining with an antibody against the HA-epitope (HA) and against acetylated tubulin also shows the presence of the truncated polycystin-2 protein in primary cilia (arrows). Given the fine structure of primary cilia, longer exposure times had to be taken to visualize the cilia, resulting in the extremely bright signal of the brush border. (c) In transfected LLC-PK_1 cells, the truncated, epitope-tagged polycystin-2 protein again is present in primary cilia (arrow) as demonstrated by double staining for the HA-epitope (HA) and acetylated tubulin. Bars = 50 μm (a) and 25 μm (b and c).

correct diameter of the tubules is maintained (for review, see references [46,47]). This prompted us to examine primary cilia in the transgenic rat kidneys more closely by scanning electron microscopy. Similar to what has been observed before in mouse kidneys (48), primary cilia of proximal tubular epithelial cells did not extend above the brush border in wild-type rat kidneys (data not shown). That primary cilia are hidden in the brush border became apparent in polycystic kidneys of transgenic rats, where primary cilia were detected in the transition zone between the intact brush border and denuded epithelium (data not shown). Furthermore, in polycystic kidneys, we occasionally observed that some cilia extended above the brush border, a phenomenon that we never noticed in wild-type rat kidneys. To find out whether the overshooting ciliary growth in proximal tubules of transgenic rats is a primary or a secondary phenomenon, we turned our attention to stably transfected LLC-PK_1 cells that inducibly produced the truncated polycystin-2 protein. In the "off" state, primary cilia had an average length of 30.4 μm (30.4 $\pm$ 14.5 μm, 1001 cilia). Upon induction of the truncated polycystin-2 protein for 3 wk, primary cilia that contained the mutant protein only grew to an average length of 21.0 μm (21.0 $\pm$ 10.7 μm, 929 cilia; $P < 0.0001$), indicating that the truncated polycystin-2 protein stunted the extension of primary cilia and that longer cilia in the transgenic rats are a secondary phenomenon.

Expression of the PKD2 (1/703) cDNA Leads to Degeneration of the Rod and Cone Layer in the Retina

In the retina, the outer segments of the rod and cone cells are connected to the inner segments through a ciliary structure (49). Remarkably, syndromes have been described whereby cystic kidney disease is associated with retinal degeneration (*e.g.*, references [50–52]); we therefore also looked for phenotypic changes in the eyes of transgenic rats. When we previously analyzed the expression pattern of the rat *Pkd2* gene, we were able to detect polycystin-2 only in the cornea (53), but because according to the UniGene database the PKD2 mRNA should be present in the retina, we carried out another immunohistochemical study, this time using microwave treatment of the sections. Indeed, we were able to detect the endogenous polycystin-2 protein in the retina (Figure 4c). Similarly, the truncated polycystin-2 protein was present in the somata and the photoreceptor segments of rod and cone cells of the transgenic rats (Figure 3, a through c). This histologic finding correlated well with the phenotypic changes that we observed in the retinas of both transgenic lines. Whereas at 1 mo of age we did not detect a difference between the retina of the transgenic and wild-type rats, the rod and cone layer of the transgenic animals had shrunk markedly at 3 mo (Figure 3, a through d). Remarkably, the degeneration of the retina was accompanied by the dishevelled appearance of microtubule-containing structures that likely represent connecting cilia (Figure 3, e and f).

Hints on the Possible Mechanism Underlying Cyst Formation

There are several possibilities for how a truncated polycystin-2 protein can induce renal cyst formation in the presence of the wild-type polycystin-2 protein. We first tested whether full-length and truncated polycystin-2 still can interact, thereby possibly forming cation channels with abnormal electrophysiologic properties. It has been shown that the COOH-terminus of polycystin-2 can interact with itself (13,14), but these earlier experiments were conducted *in vitro*, in yeast and in mammalian cells, using fusion proteins with only the COOH-terminus of polycystin-2. So far, a homomeric interaction has not been demonstrated for the full-length polycystin-2 protein in mam-

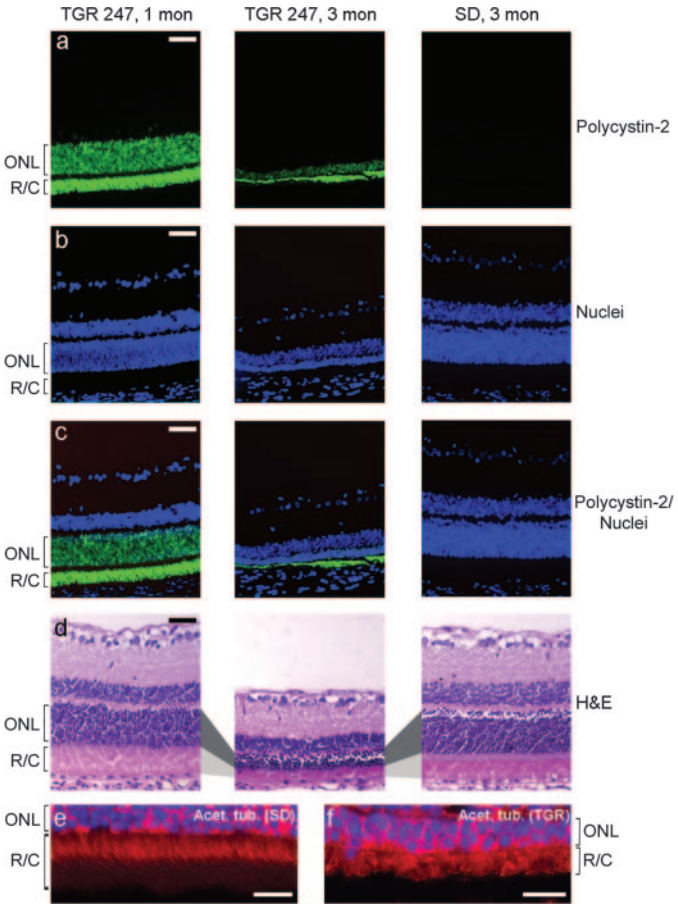

Figure 3. Retinal degeneration in transgenic line 247. Immunohistochemistry (a) with an anti-HA antibody localizes the HA-epitope–tagged truncated polycystin-2 protein to the outer nuclear layer (ONL) and the rod and cone layer (R/C) as demonstrated by counterstaining the nuclei with 4′,6-diamidino-2-phenylindole dihydrochloride (b; merged in c). (d) By hematoxylin and eosin staining, it can be appreciated easily that the ONL and the R/C of the retina have shrunk in 3-mo-old transgenic rats. (e and f) Staining for acetylated tubulin demonstrates the parallel arrangement of connecting cilia in the retinas of normal SD rats and the dishevelled appearance of microtubule-containing structures in the degenerated retina of transgenic line 247 (TGR). Bars = 50 μm (a through d) and 20 μm (e and f).

malian cells; furthermore, it is not known whether other domains in polycystin-2 also can mediate a homomeric interaction. By establishing stably transfected cells that produce a His-tagged full-length polycystin-2 protein together with either an HA-tagged full-length or an HA-tagged truncated polycystin-2 protein, we were able to demonstrate a homomeric interaction for the full-length polycystin-2 protein but not between the truncated and the full-length protein (Figure 4a). Therefore, the self-interaction of full-length polycystin-2 should not be prevented by the truncated protein, and functional polycystin-2 channels still should be allowed to form. Another explanation for the phenotypic changes in the transgenic rats could be a transgene-induced mislocalization of the endogenous polycystin-2 protein or a change in the levels of the endogenous rat Pkd2 mRNA. However, in both the wild-type and the transgenic rats, the endogenous polycystin-2 protein still was present in the basal compartment and in cilia of proximal tubular epithelial cells (Figure 4, b, d, and e) and in retinal photoreceptor cells (Figure 4, c and f). Furthermore, both in the eyes and in the kidneys, the levels of the endogenous Pkd2 mRNA were the same in wild-type and transgenic rats as determined by RNase protection assay (data not shown).

Because the truncated polycystin-2 protein obviously did not affect the full-length polycystin-2 protein directly, we next sought to find evidence of whether the mutant protein had an effect on intracellular calcium levels. Several reports have argued that the activation of purinergic receptors through ATP increases the secretory activity of cyst wall epithelia (54–56). We therefore examined how stably transfected LLC-PK$_1$ cells that inducibly produced either full-length or the truncated polycystin-2 protein reacted to ATP. Whereas induction of the full-length protein enhanced the Ca^{2+} response of LLC-PK$_1$ cells to ATP as judged by the peak of the $[Ca^{2+}]_i$, the synthesis of the truncated polycystin-2 protein did not change the $[Ca^{2+}]_i$ after stimulation of the cells with ATP (Figure 5a). Because in LLC-PK$_1$ cells we have localized the full-length polycystin-2 protein to the endoplasmic reticulum, we also measured the release of Ca^{2+} from intracellular stores by exposing LLC-PK$_1$ cells to the Ca^{2+} ionophore ionomycin. Remarkably, LLC-PK$_1$ cells that produced the truncated polycystin-2 protein released less Ca^{2+} into the cytoplasm, thereby indicating that the endoplasmic reticulum contained less Ca^{2+} (Figure 5b).

Discussion

We have generated a new rat model of ADPKD by expressing a truncated human polycystin-2 cDNA in Sprague-Dawley rats. Although we used the widely active CMV promoter to drive the transgenic expression cassette and although we observed expression in a large number of tissues, no histologic abnormalities were detected in most tissues. Whether this observation is due to the high expression levels of the transgenic cassette in the kidney or emphasizes the particular sensitivity of some tissues to the mutated polycystin-2 protein remains an open question for now. It also was surprising to see that in both transgenic lines the transgenic cassette was expressed predominantly in proximal tubules, for which we have no explanation. We want to point out, however, that cysts have been observed regularly in proximal tubules of patients (57–61) and that therefore our transgenic rats do not differ from the human disease in this respect.

A cystic phenotype in two independent transgenic lines strongly supports the argument that the overexpression of the truncated polycystin-2 cDNA is responsible for the kidney damage and argues against the hypothesis that the integration of the transgenic cassette into a specific locus leads to the formation of cysts. Similar to what has been observed in human ADPKD, the transgenic rats developed fibrosis and showed focal cyst formation. Although an explanation for the latter could be the known mosaic activity of the CMV promoter, we cannot rule out other factors, such as a particular microenvi-

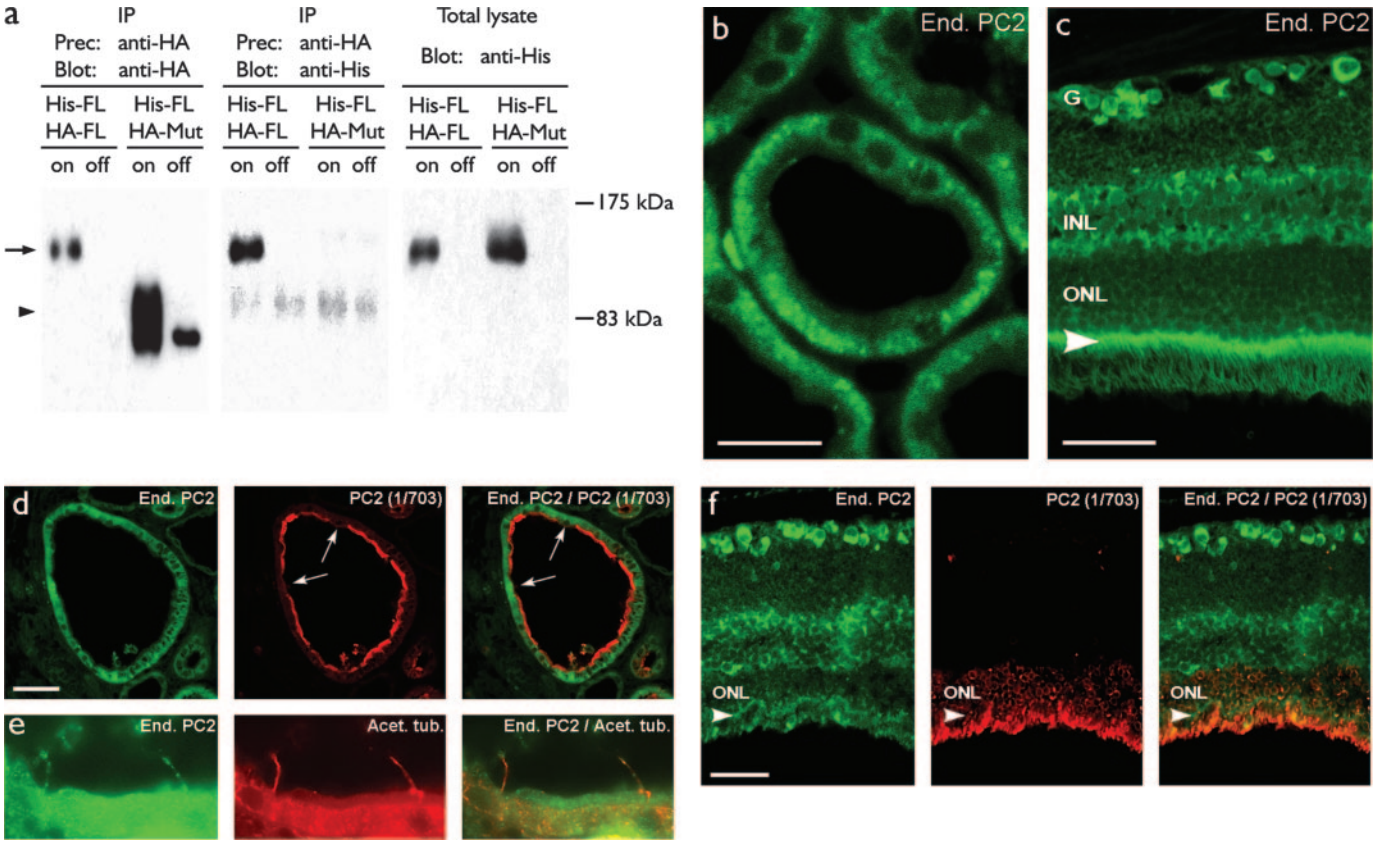

Figure 4. Interaction between full-length and truncated polycystin-2, and distribution of the endogenous polycystin-2 protein in transgenic rats. (a) Immunoprecipitations (IP) were performed with stably transfected HeLa cells that inducibly produced either histidine- and HA-epitope–tagged full-length polycystin-2 (left side of each panel) or histidine-tagged full-length and HA-epitope–tagged truncated polycystin-2 proteins (right side of each panel). IP and subsequent incubation of the Western blot with the anti–HA-epitope antibody demonstrates the expression of the HA-epitope–tagged full-length and truncated polycystin-2 proteins (left; to correct for the different expression levels, 10 μg of total protein was used in the case of the full-length protein and 100 μg of total protein in the case of the truncated protein). When the IP was carried out with the anti–HA-epitope antibody and the Western blot was incubated with the anti–histidine-tail antibody, it becomes evident that only the full-length proteins interact with each other (middle; to correct for the different expression levels of the HA-epitope–tagged polycystin-2 proteins, 90 μg of total protein was used in the case of the full-length protein and 900 μg of total protein in the case of the truncated protein). The synthesis of the histidine-tagged full-length polycystin-2 protein was demonstrated by analysis of total cell lysate with the anti–histidine-tail antibody (right; 8 μg of total protein was loaded when the full-length proteins were coexpressed, and 30 μg of total protein was loaded when the full-length and truncated proteins were coexpressed). Arrow, full-length polycystin-2; arrowhead, truncated polycystin-2. (b) The endogenous polycystin-2 protein in a wild-type SD rat is located in the basal compartment of proximal tubular epithelial cells. (c) In the retina of a normal SD rat, the endogenous polycystin-2 was present in the ganglion cell layer (G), the inner nuclear layer (INL), the ONL, and the R/C of the photoreceptor cells (the arrowhead points to the presumable inner segment of the photoreceptor cells). (d and e) In cyst wall cells, the endogenous polycystin-2 protein (green) still is present in the basal compartment (d) and in cilia (e), whereas the truncated polycystin-2 (red) is detected in the brush border (d). The arrows in d point to two areas where the truncated protein is absent. (f) In the retina of transgenic rats, the endogenous polycystin-2 protein (green) still was synthesized in the dysmorphic R/C of the photoreceptor cells, whereas the truncated polycystin-2 (red) is detected in the ONL and the R/C (the arrowhead points to the presumable inner segment of the photoreceptor cells). Bars = 25 μm (b) and 50 μm (c through f).

ronment. We were surprised by the variability of disease severity between animals. It has to be remembered, however, that the transgenic rats were established on a Sprague-Dawley background, which is an outbred rat strain, and that the genetic background of the various animals therefore probably is heterogeneous. Crosses are under way to transfer the transgene into an inbred rat strain to determine more precisely the effect of the genetic background.

It has been estimated that renal cysts in patients with ADPKD develop in only approximately 5% of the nephrons. This observation is puzzling in light of the dominant inheritance of the disease, but it can be explained by the two-hit hypothesis, which in analogy to the action of tumor suppressor genes states that a second somatic mutation is required for cyst formation (28). Support for this mechanism has been gained from a mouse model, in which an unstable *Pkd2* allele was

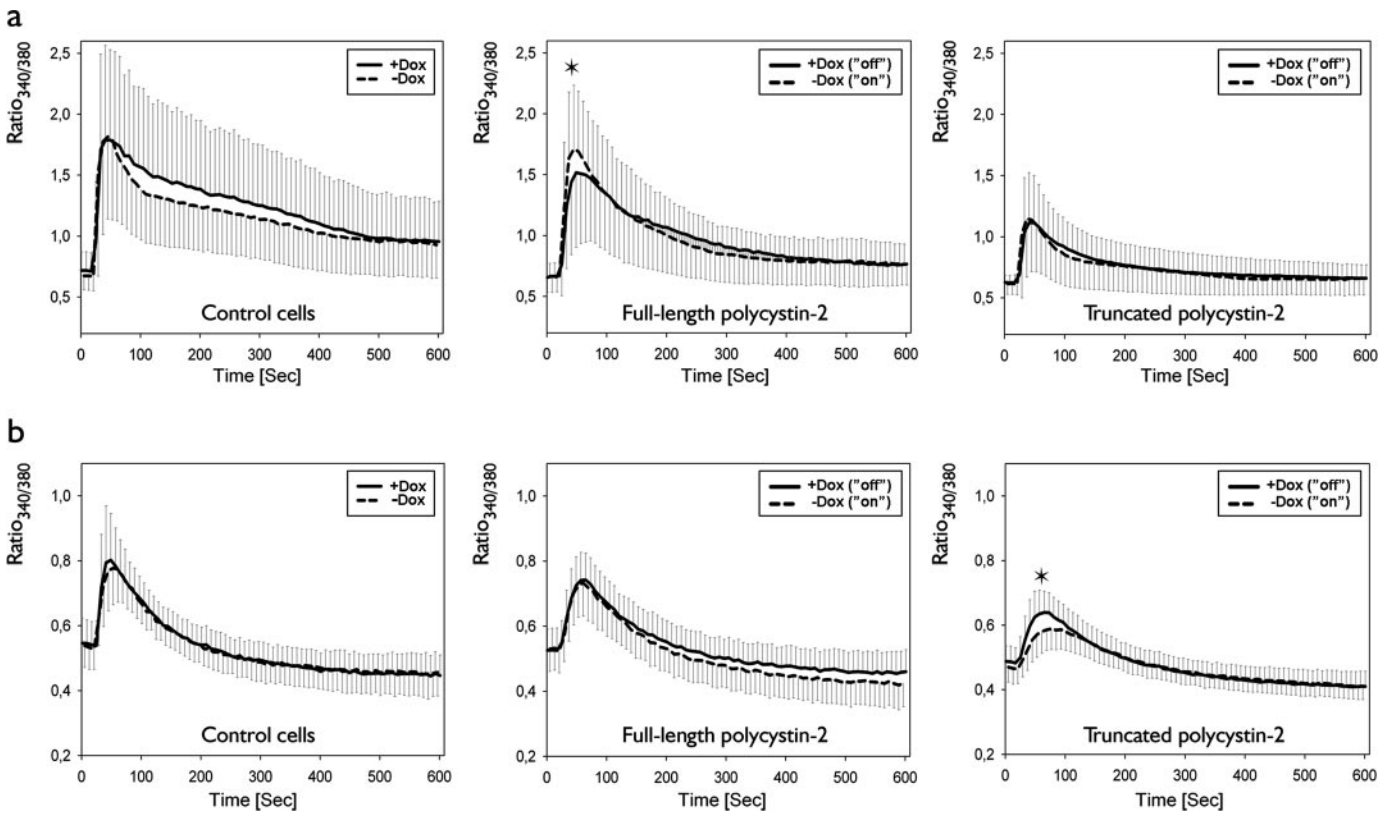

Figure 5. Ca^{2+} response and intracellular Ca^{2+} stores in LLC-PK_1 cells that inducibly produced the truncated polycystin-2 protein. (a) Stably transfected LLC-PK_1 cells that inducibly produced either a HA-tagged full-length or truncated polycystin-2 protein were stimulated with 10 μM ATP at 20 s into the experiment. The induction of the full-length polycystin-2 protein by removing doxycycline led to a higher $[Ca^{2+}]_i$ peak, whereas the induction of the truncated polycystin-2 protein had no effect on the $[Ca^{2+}]_i$. The parent cell line (control cells), which was grown in the absence and presence of doxycycline, was used as a negative control. (b) For determination of the status of the intracellular Ca^{2+} stores, the stably transfected LLC-PK_1 cells were incubated in Ca^{2+}-free buffer and then exposed to 10 μM ionomycin at 20 s into the experiment. In cells that produced the truncated polycystin-2 protein, the stores were less filled, but no difference was seen when the full-length polycystin-2 protein was induced. Again, the parent cell line, grown in the absence and presence of doxycycline, was used as a negative control. Shown are the mean and the SD. *$P <$ 0.001 for peak $[Ca^{2+}]_i$.

introduced into the germline that can undergo somatic recombination to form a null allele (29,30). Therefore, although the pattern of inheritance is dominant, the disease behaves in a recessive manner on a cellular level, and such a scenario could explain easily the focal nature of cyst formation and the slowly progressive course of the disease, which usually takes decades before it leads to end-stage renal failure. There are some open questions regarding the two-hit hypothesis, however, such as why a somatic mutation in the second allele has not been found in 100% of the cysts examined, why polycystin-2 still was detected by immunohistochemistry in many cyst-lining epithelial cells (see references in [6]), and why in the *cpk/cpk* mouse model of autosomal recessive polycystic kidney disease cysts also develop focally (62,63). Although our results certainly do not contradict the two-hit hypothesis, they suggest an additional mechanism of cystogenesis by attributing a role to the mutated polycystin-2 protein. Such a hypothesis is supported by the finding that LLC-PK_1 cells elaborate shorter cilia in the presence of the mutated polycystin-2 protein. Consistent with this *in vitro* result is the degeneration of the retinal photoreceptor cells, whereas the overshooting ciliary growth that we observed on some cyst-lining epithelial cells has to be considered a secondary phenomenon.

The full-length polycystin-2 protein has the characteristics of a high-conductance, Ca^{2+}-modulated cation channel that is permeable to mono- and divalent ions, whereas the 703–amino acid mutant protein, which was used in this study, still has some channel activity but no longer responds to Ca^{2+} (35). Because the wild-type and the truncated polycystin-2 proteins no longer can interact, a direct modulation of the full-length by the truncated polycystin-2 protein is unlikely; rather, the truncated polycystin-2 protein may cause cyst formation by acting as a dysregulated channel in itself. However, we cannot rule out that precise polycystin-2 levels have to be maintained and that overexpression of the mutant PKD2 cDNA *per se* leads to cyst formation. In the case of polycystin-1, there is precedence that levels of polycystin-1 that are both too low (64,65) and too high (66,67) lead to the development of polycystic kidneys. Additional copies of a *PKD* gene therefore can result in cyst formation, and further

experiments, such as a knock-in approach, are necessary to decide whether cyst formation in our transgenic rats results from an abnormal biologic activity of the truncated protein (*e.g.*, by a dominant negative mechanism) or simply is due to the high levels of the mutant polycystin-2 protein. If the first hypothesis is correct, then gene therapy that is based on the introduction of the wild-type protein is unlikely to succeed because it will not affect the mutant protein.

Acknowledgments

Financial support from the European Union (QLRT-2000-01104) and from the German Research Council (SFB 699) are gratefully acknowledged.

The human PKD2 cDNA was kindly provided by Stefan Somlo. We thank Dr. Kálmán Szabó for expert help in taking the scanning electron micrographs. Karin Spies and Jutta Christophel skillfully determined the serum and urine parameters. We also are thankful to Ton Maurer for photographic work and arrangement of the figures.

References

1. Dalgaard OZ: Bilateral polycystic disease of the kidneys. A follow-up of two hundred and eighty-four patients and their families. *Acta Med Scand* 328[Suppl]: 2–31, 1957
2. Iglesias CG, Torres VE, Offord KP, Holley KE, Beard CM, Kurland LT: Epidemiology of adult polycystic kidney disease, Olmsted County, Minnesota: 1935–1980. *Am J Kidney Dis* 2: 630–639, 1983
3. Churchill DN, Bear JC, Morgan J, Payne RH, McManamon PJ, Gault MH: Prognosis of adult onset polycystic kidney disease re-evaluated. *Kidney Int* 26: 190–193, 1984
4. Parfrey PS, Bear JC, Morgan J, Cramer BC, McManamon PJ, Gault MH, Churchill DN, Singh M, Hewitt R, Somlo S, Reeders ST: The diagnosis and prognosis of autosomal dominant polycystic kidney disease. *N Engl J Med* 323: 1085–1090, 1990
5. Gabow PA, Johnson AM, Kaehny WD, Kimberling WJ, Lezotte DC, Duley IT, Jones RH: Factors affecting the progression of renal disease in autosomal-dominant polycystic kidney disease. *Kidney Int* 41: 1311–1319, 1992
6. Gallagher AR, Hidaka S, Gretz N, Witzgall R: Molecular basis of autosomal-dominant polycystic kidney disease. *Cell Mol Life Sci* 59: 682–693, 2002
7. Peters DJM, Sandkuijl LA: Genetic heterogeneity of polycystic kidney disease in Europe. *Contrib Nephrol* 97: 128–139, 1992
8. Roscoe JM, Brissenden JE, Williams EA, Chery AL, Silverman M: Autosomal dominant polycystic kidney disease in Toronto. *Kidney Int* 44: 1101–1108, 1993
9. Wright AF, Teague PW, Pound SE, Pignatelli PM, Macnicol AM, Carothers AD, de Mey RJ, Allan PL, Watson ML: A study of genetic linkage heterogeneity in 35 adult-onset polycystic kidney disease families. *Hum Genet* 90: 569–571, 1993
10. Torra R, Badenas C, Darnell A, Nicolau C, Volpini V, Revert L, Estivill X: Linkage, clinical features, and prognosis of autosomal dominant polycystic kidney disease types 1 and 2. *J Am Soc Nephrol* 7: 2142–2151, 1996
11. Mochizuki T, Wu G, Hayashi T, Xenophontos SL, Veldhuisen B, Saris JJ, Reynolds DM, Cai Y, Gabow PA, Pierides A, Kimberling WJ, Breuning MH, Deltas CC, Peters DJM, Somlo S: PKD2, a gene for polycystic kidney disease that encodes an integral membrane protein. *Science* 272: 1339–1342, 1996
12. Delmas P, Padilla F, Osorio N, Coste B, Raoux M, Crest M: Polycystins, calcium signaling, and human diseases. *Biochem Biophys Res Commun* 322: 1374–1383, 2004
13. Qian F, Germino FJ, Cai Y, Zhang X, Somlo S, Germino GG: PKD1 interacts with PKD2 through a probable coiled-coil domain. *Nat Genet* 16: 179–183, 1997
14. Tsiokas L, Kim E, Arnould T, Sukhatme VP, Walz G: Homo- and heterodimeric interactions between the gene products of *PKD1* and *PKD2. Proc Natl Acad Sci U S A* 94: 6965–6970, 1997
15. Li Q, Montalbetti N, Shen PY, Dai X-Q, Cheeseman CI, Karpinski E, Wu G, Cantiello HF, Chen X-Z: Alpha-actinin associates with polycystin-2 and regulates its channel activity. *Hum Mol Genet* 14: 1587–1603, 2005
16. Lehtonen S, Ora A, Olkkonen VM, Geng L, Zerial M, Somlo S, Lehtonen E: In vivo interaction of the adapter protein CD2-associated protein with the type 2 polycystic kidney disease protein, polycystin-2. *J Biol Chem* 275: 32888–32893, 2000
17. Rundle DR, Gorbsky G, Tsiokas L: PKD2 interacts and co-localizes with mDia1 to mitotic spindles of dividing cells. Role of mDia1 in PKD2 localization to mitotic spindles. *J Biol Chem* 279: 29728–29739, 2004
18. Li X, Luo Y, Starremans PG, McNamara CA, Pai Y, Zhou J: Polycystin-1 and polycystin-2 regulate the cell cycle through the helix-loop-helix inhibitor Id2. *Nat Cell Biol* 7: 1202–1212, 2005
19. Li Y, Wright JM, Qian F, Germino GG, Guggino WB: Polycystin 2 interacts with type I inositol 1,4,5-trisphosphate receptor to modulate intracellular Ca2+ signaling. *J Biol Chem* 280: 41298–41306, 2005
20. Kottgen M, Benzing T, Simmen T, Tauber R, Buchholz B, Feliciangeli S, Huber TB, Schermer B, Kramer-Zucker A, Hopker K, Simmen KC, Tschucke CC, Sandford R, Kim E, Thomas g, Walz G: Trafficking of TRPP2 by PACS proteins represents a novel mechanism of ion channel regulation. *EMBO J* 24: 705–716, 2005
21. Hidaka S, Konecke V, Osten L, Witzgall R: PIGEA-14, a novel coiled-coil protein affecting the intracellular distribution of polycystin-2. *J Biol Chem* 279: 35009–35016, 2004
22. Li Q, Dai Y, Guo L, Liu Y, Hao C, Wu G, Basora N, Michalak M, Chen X-Z: Polycystin-2 associates with tropomyosin-1, an actin microfilament component. *J Mol Biol* 325: 949–962, 2003
23. Li Q, Shen PY, Wu G, Chen X-Z: Polycystin-2 interacts with troponin I, an angiogenesis inhibitor. *Biochemistry* 42: 450–457, 2003
24. Tsiokas L, Arnould T, Zhu C, Kim E, Walz G, Sukhatme VP: Specific association of the gene product of *PKD2* with the TRPC1 channel. *Proc Natl Acad Sci U S A* 96: 3934–3939, 1999
25. Witzgall R: Polycystin-2: An intracellular or plasma membrane channel? *Naunyn-Schmiedebergs Arch Pharmacol* 371: 342–347, 2005
26. Pazour GJ, San Agustin JT, Follit JA, Rosenbaum JL, Witman GB: Polycystin-2 localizes to kidney cilia and the

ciliary level is elevated in orpk mice with polycystic kidney disease. *Curr Biol* 12: R378–R380, 2002
27. Yoder BK, Hou X, Guay-Woodford LM: The polycystic kidney disease proteins, polycystin-1, polycystin-2, polaris, and cystin, are co-localized in renal cilia. *J Am Soc Nephrol* 13: 2508–2516, 2002
28. Pei Y: A 'two-hit' model of cystogenesis in autosomal dominant polycystic kidney disease. *Trends Mol Med* 7: 151–156, 2001
29. Wu G, D'Agati V, Cai Y, Markowitz G, Park JH, Reynolds DM, Maeda Y, Le TC, Hou H Jr, Kucherlapati R, Edelmann W, Somlo S: Somatic inactivation of Pkd2 results in polycystic kidney disease. *Cell* 93: 177–188, 1998
30. Thomson RB, Mentone S, Kim R, Earle K, Delpire E, Somlo S, Aronson PS: Histopathological analysis of renal cystic epithelia in the Pkd2WS25/− mouse model of ADPKD. *Am J Physiol Renal Physiol* 285: F870–F880, 2003
31. Koptides M, Mean R, Demetriou K, Pierides A, Deltas CC: Genetic evidence for a trans-heterozygous model for cystogenesis in autosomal dominant polycystic kidney disease. *Hum Mol Genet* 9: 447–452, 2000
32. Watnick T, He N, Wang K, Liang Y, Parfrey P, Hefferton D, St. George-Hyslop P, Germino G, Pei Y: Mutations of PKD1 in ADPKD2 cysts suggest a pathogenic effect of trans-heterozygous mutations. *Nat Genet* 25: 143–144, 2000
33. Ausubel FA, Brent R, Kingston RE, Moore DD, Seidman JG, Smith JA, Struhl K: *Current Protocols in Molecular Biology*, New York, John Wiley & Sons, 1996
34. Gossen M, Bujard H: Tight control of gene expression in mammalian cells by tetracycline-responsive promoters. *Proc Natl Acad Sci U S A* 89: 5547–5551, 1992
35. Koulen P, Cai Y, Geng L, Maeda Y, Nishimura S, Witzgall R, Ehrlich BE, Somlo S: Polycystin-2 is an intracellular calcium release channel. *Nat Cell Biol* 4: 191–197, 2002
36. Morgenstern JP, Land H: Advanced mammalian gene transfer: High titre retroviral vectors with multiple drug selection markers and a complementary helper-free packaging cell line. *Nucleic Acids Res* 18: 3587–3596, 1990
37. Chen C, Okayama H: High-efficiency transformation of mammalian cells by plasmid DNA. *Mol Cell Biol* 7: 2745–2752, 1987
38. Cockett MI, Ochalski R, Benwell K, Franco R, Wardwell-Swanson J: Simultaneous expression of multi-subunit proteins in mammalian cells using a convenient set of mammalian cell expression vectors. *Biotechniques* 23: 402–407, 1997
39. Dong Y, Skoultchi AI, Pollard JW: Efficient DNA transfection of quiescent mammalian cells using poly-L-ornithine. *Nucleic Acids Res* 21: 771–772, 1993
40. Hartel-Schenk S, Gossrau R, Reutter W: Comparative immunohistochemistry and histochemistry of dipeptidyl peptidase IV in rat organs during development. *Histochem J* 22: 567–578, 1990
41. Cai Y, Maeda Y, Cedzich A, Torres VE, Wu G, Hayashi T, Mochizuki T, Park JH, Witzgall R, Somlo S: Identification and characterization of polycystin-2, the PKD2 gene product. *J Biol Chem* 274: 28557–28565, 1999
42. Karniski LP, Lotscher M, Fucentese M, Hilfiker H, Biber J, Murer H: Immunolocalization of sat-1 sulfate/oxalate/bicarbonate anion exchanger in the rat kidney. *Am J Physiol* 275: F79–F87, 1998
43. Chomczynski P, Sacchi N: Single-step method of RNA isolation by acid guanidinium thiocyanate-phenol-chloroform extraction. *Anal Biochem* 162: 156–159, 1987
44. Zor T, Selinger Z: Linearization of the Bradford protein assay increases its sensitivity: Theoretical and experimental studies. *Anal Biochem* 236: 302–308, 1996
45. Deltas CC: Mutations of the human polycystic kidney disease 2 (PKD2) gene. *Hum Mutat* 18: 13–24, 2001
46. Pazour GJ: Intraflagellar transport and cilia-dependent renal disease: The ciliary hypothesis of polycystic kidney disease. *J Am Soc Nephrol* 15: 2528–2536, 2004
47. Witzgall R: New developments in the field of cystic kidney diseases. *Curr Mol Med* 5: 455–465, 2005
48. Brown NE, Murcia NS: Delayed cystogenesis and increased ciliogenesis associated with the re-expression of polaris in Tg737 mutant mice. *Kidney Int* 63: 1220–1229, 2003
49. Standring S: *Gray's Anatomy*, 39th Ed., Edinburgh, Elsevier Churchill Livingstone, 2005
50. Katsanis N, Beales PL, Woods MO, Lewis RA, Green JS, Parfrey PS, Ansley SJ, Davidson WS, Lupski JR: Mutations in MKKS cause obesity, retinal dystrophy and renal malformations associated with Bardet-Biedl syndrome. *Nat Genet* 26: 67–70, 2000
51. Olbrich H, Fliegauf M, Hoefele J, Kispert A, Otto E, Volz A, Wolf MT, Sasmaz G, Trauer U, Reinhardt R, Sudbrak R, Antignac C, Gretz N, Walz G, Schermer B, Benzing T, Hildebrandt F, Omran H: Mutations in a novel gene, NPHP3, cause adolescent nephronophthisis, tapeto-retinal degeneration and hepatic fibrosis. *Nat Genet* 34: 455–459, 2003
52. Otto EA, Loeys B, Khanna H, Hellemans J, Sudbrak R, Fan S, Muerb U, O'Toole JF, Helou J, Attanasio M, Utsch B, Sayer JA, Lillo C, Jimeno D, Coucke P, de Paepe A, Reinhardt R, Klages S, Tsuda M, Kawakami I, Kusakabe T, Omran H, Imm A, Tippens M, Raymond PA, Hill J, Beales P, He S, Kispert A, Margolis B, Williams DS, Swaroop A, Hildebrandt F: Nephrocystin-5, a ciliary IQ domain protein, is mutated in Senior-Loken syndrome and interacts with RPGR and calmodulin. *Nat Genet* 37: 282–288, 2005
53. Obermuller N, Gallagher AR, Cai Y, Gassler N, Gretz N, Somlo S, Witzgall R: The rat Pkd2 protein assumes distinct subcellular distributions in different organs. *Am J Physiol* 277: F914–F925, 1999
54. Wilson PD, Hovater JS, Casey CC, Fortenberry JA, Schwiebert EM: ATP release mechanisms in primary cultures of epithelia derived from the cysts of polycystic kidneys. *J Am Soc Nephrol* 10: 218–229, 1999
55. Schwiebert EM, Wallace DP, Braunstein GM, King SR, Peti-Peterdi J, Hanaoka K, Guggino WB, Guay-Woodford LM, Bell PD, Sullivan LP, Grantham JJ, Taylor AL: Autocrine extracellular purinergic signaling in epithelial cells derived from polycystic kidneys. *Am J Physiol Renal Physiol* 282: F763–F775, 2002
56. Hooper KM, Unwin RJ, Sutters M: The isolated C-terminus of polycystin-1 promotes increased ATP-stimulated chloride secretion in a collecting duct cell line. *Clin Sci* 104: 217–221, 2003
57. Grantham JJ, Geiser JL, Evan AP: Cyst formation and growth in autosomal dominant polycystic kidney disease. *Kidney Int* 31: 1145–1152, 1987

58. Devuyst O, Burrow CR, Smith BL, Agre P, Knepper MA, Wilson PD: Expression of aquaporins-1 and -2 during nephrogenesis and in autosomal dominant polycystic kidney disease. *Am J Physiol* 271: F169–F183, 1996
59. Bachinsky DR, Sabolic I, Emmanouel DS, Jefferson DM, Carone FA, Brown D, Perrone RD: Water channel expression in human ADPKD kidneys. *Am J Physiol* 268: F398–F403, 1995
60. Verani R, Walker P, Silva FG: Renal cystic disease of infancy: Results of histochemical studies. *Pediatr Nephrol* 3: 37–42, 1989
61. Baert L: Hereditary polycystic kidney disease (adult form): A microdissection study of two cases at an early stage of the disease. *Kidney Int* 13: 519–525, 1978
62. Avner ED, Studnicki FE, Young MC, Sweeney WE Jr, Piesco NP, Ellis D, Fettermann GH: Congenital murine polycystic kidney disease. I. The ontogeny of tubular cyst formation. *Pediatr Nephrol* 1: 587–596, 1987
63. Gattone VH II, Calvet JP, Cowley BD Jr, Evan AP, Shaver TS, Helmstadter K, Grantham JJ: Autosomal recessive polycystic kidney disease in a murine model. A gross and microscopic description. *Lab Invest* 59: 231–238, 1988
64. Lantinga-van Leeuwen IS, Dauwerse JG, Baelde HJ, Leonhard WN, van de Wal A, Ward CJ, Verbeek S, DeRuiter MC, Breuning MH, de Heer E, Peters DJM: Lowering of Pkd1 expression is sufficient to cause polycystic kidney disease. *Hum Mol Genet* 13: 3069–3077, 2004
65. Jiang S-T, Chiou Y-Y, Wang E, Lin H-K, Lin Y-T, Chi Y-C, Wang C-KL, Tang M-J, Li H: Defining a link with autosomal-dominant polycystic kidney disease in mice with congenitally low expression of *Pkd1*. *Am J Pathol* 168: 205–220, 2006
66. Pritchard L, Sloane-Stanley JA, Sharpe JA, Aspinwall R, Lu W, Buckle V, Strmecki L, Walker D, Ward CJ, Alpers CE, Zhou J, Wood WG, Harris PC: A human PKD1 transgene generates functional polycystin-1 in mice and is associated with a cystic phenotype. *Hum Mol Genet* 9: 2617–2627, 2000
67. Thivierge C, Kurbegovic A, Couillard M, Guillaume R, Cote O, Trudel M: Overexpression of PKD1 causes polycystic kidney disease. *Mol Cell Biol* 26: 1538–1548, 2006

Supplemental information for this article is available online at http://www.jasn.org.